Large mixing ratios of atmospheric nitrous acid (HONO) at Concordia (East Antarctic plateau) in summer: A strong source from surface snow?

Michel Legrand[1,2], Susanne Preunkert[1,2], Markus Frey[3], Thorsten Bartels-Rausch[4], Alexandre Kukui[5,6], Martin D. King[7], Joel Savarino[1,2], Michael Kerbrat[1,2], and Bruno Jourdain[1,2]

[1] Univ. Grenoble Alpes, LGGE, F-38000 Grenoble, France

[2] CNRS, LGGE, F-38000 Grenoble, France

CNRS/Univ. Grenoble Alpes, Laboratoire de Glaciologie et Géophysique de l'Environnement (LGGE) UMR 5183, Grenoble, F-38041, France

[3] British Antarctic Survey (BAS), Natural Environment Research Council, Cambridge, UK

[4] Laboratory of Radio and Environmental Chemistry, Paul Scherrer Institute (PSI), 5232 Villigen, Switzerland

[5] Laboratoire des Atmosphères, Milieux, Observations Spatiales (LATMOS), Paris, France

[6] Laboratoire de Physique et Chimie de l'Environnement et de l'Espace (LPC2E) UMR-CNRS, Orléans, France

[7] Department of Earth Sciences, Royal Holloway University of London, Egham, Surrey, TW20 0EX, UK

Correspondence email: Legrand@lgge.obs.ujf-grenoble.fr

Abstract

During the austral summer 2011/2012 atmospheric nitrous acid was investigated for the second time at the Concordia site (75°06'S, 123°33'E) located on the East Antarctic plateau by deploying a long path absorption photometer (LOPAP). Hourly mixing ratios of HONO measured in December 2011/January 2012 (35 ± 5.0 pptv) were similar to those measured in December 2010/January 2011 (30.4 ± 3.5 pptv). The large value of the HONO mixing ratio at the remote Concordia site suggests a local source of HONO in addition to weak production from oxidation of NO by the OH radical. Laboratory experiments demonstrate that surface snow removed from Concordia can produce gas phase HONO at mixing ratios half that of NO_x mixing ratio produced in the same experiment at typical temperatures encountered at Concordia in summer. Using these lab data and the emission flux of NO_x from snow

estimated from the vertical gradient of atmospheric concentrations measured during the campaign, a mean diurnal HONO snow emission ranging between 0.5 and 0.8×10^9 molecules cm^{-2} s^{-1} is calculated. Model calculations indicate that, in addition to around 1.2 pptv of HONO produced by the NO oxidation, these HONO snow emissions can only explain 6.5 to 10.5 pptv of HONO in the atmosphere at Concordia. To explain the difference between observed and simulated HONO mixing ratios, tests were done both in the field and at lab to explore the possibility that the presence of HNO_4 had biased the measurements of HONO.

1. Introduction

The existence of an oxidizing boundary layer over the Antarctic continent was first highlighted by measurements carried out at the South Pole, where a mean concentration of 2.5×10^6 OH radicals cm^{-3} was observed (Mauldin et al., 2001a), making the South Pole atmospheric boundary layer as oxidative as the remote tropical marine boundary layer (Mauldin et al., 2001b). Chen et al. (2001) and Davis et al. (2001) showed that the presence of high concentrations of NO_x produced by the photolysis of nitrate present in surface snow permits the required efficient recycling of HO_2 into OH. Aside from snow photochemical emission of NO_x that acts as a secondary source of OH, the role of HONO as a primary source of OH remains unclear. Using a mist chamber followed by ion chromatography analysis of nitrite, Dibb et al. (2004) reported a median HONO mixing ratio close to 30 pptv at the South Pole. However, follow-up measurements by laser-induced fluorescence (LIF) indicated lower mixing ratios (6 pptv on average) and an interference with HNO_4 has been suspected (Liao et al., 2006). Furthermore, as discussed by Chen et al. (2004) the consideration of 30 pptv of HONO in the lower atmosphere over the South Pole leads to an OH over-prediction by gas-phase photochemical models by a factor of 3 to 5. The authors questioned whether the discrepancy between observed and simulated concentrations of OH at the South Pole was due to measurements of HONO suffering from overestimation due to chemical interferences or if the mechanisms of the model missed HO_x and NO_x losses.

Even at the level of a few pptv, the presence of HONO requires a source other than the gas-phase reaction of NO with OH and many studies measuring HONO in atmospheres overlying snow covered regions suspected HONO to be emitted from the surface snow in addition to NO_x (see Grannas et al. (2007) for a review). It has to be emphasized that most of the studies of HONO have concerned high (Arctic, Greenland) and mid (Colorado and Alps) northern latitudes where, in relation to the chemical composition of snow, the involved HONO production processes would be very different compared to the case of Antarctica.

Concerning Antarctic snow, following the pioneering shading experiment done by Jones et al. (2000) on snow from the coastal Antarctic site of Neumayer, numerous studies investigated the release of NO_x from the snow (see references in Frey et al., this issue), but only two studies reported on HONO snow emissions and none of them examined together HONO and NO_x emissions. Beine et al. (2006) reported small HONO fluxes ($3x10^7$ molecule cm^{-2} s^{-1}) above the Browning Pass (coastal Antarctic) snowpack. However, the snow chemical composition at that site is very atypical with a large presence of calcium (up to 4 ppm) attributed to the presence of a lot of rock out-crops at the site. As a consequence, even if nitrate is abundant (typically 200 ppb in fresh snow and more than 1 ppm in aged snow), the snow from that site appears to be weakly acidic and sometimes alkaline. Finally a few investigations of the vertical distribution of HONO were made at the South Pole (Dibb et al., 2004) but no fluxes were calculated. These previous Antarctic studies of HONO were using either mist chambers (Dibb et al., 2002) or high-performance liquid chromatography techniques (Beine et al., 2006). These "wet chemical instruments" sample HONO on humid or aqueous surfaces followed by analysis of the nitrite ion. However, it is well known that many heterogeneous reactions lead to the formation of nitrite on similar surfaces (Gutzwiller et al., 2002, Liao et al., 2006). In addition to these chemical interferences, it is also known that HONO can decompose or be formed on various surfaces (Chan et al., 1976). That may affect data when sampling lines of up to 30 m length were used for polar measurements (see, e.g., Beine et al., 2006).

Motivated by a strong need to extend investigations of the oxidation capacity of the lower atmosphere at the scale of the whole Antarctic continent, the OPALE (Oxidant Production over Antarctic Land and its Export) project was initiated at the end of 2010 in East Antarctica. The first OPALE campaign was conducted during austral summer 2010/2011 at the coastal site of Dumont D'Urville (Preunkert et al., 2012) and focused on OH and RO_2 measurements (Kukui et al., 2012). During this first campaign, preliminary investigations of HONO were performed at the continental site of Concordia (also denoted DC, 3233 m above sea level). In spite of the use of a long path absorption photometer (LOPAP), thought to avoid all known artefacts, high mixing ratios of HONO were observed (from 5 to 59 pptv, Kerbrat et al., 2012). In the framework of the OPALE project, a second summer campaign (2011-2012) was conducted at DC with simultaneous measurements of HONO, NO, NO_2, OH and RO_2 that are discussed in a set of companion papers of which this is one.

The paper presented here focuses on HONO data gained during the second campaign at DC. It also reports on snow irradiation experiments conducted in the laboratory at British

Antarctic Survey (BAS) on surface snow samples collected at Concordia in view to quantify a possible photochemical snow source of HONO. This was done by measuring simultaneously HONO with the LOPAP, NO and NO_2 with a 2-channel chemiluminescence detector. From these data we crudely estimate the amount of HONO released from snow within the lower atmosphere at Concordia on the basis of the NO_x snow emissions derived from the vertical gradient of atmospheric concentrations measured during the campaign by Frey et al. (this issue). The derived values of the HONO flux were used in 1D modeling calculations to evaluate the contribution of this snow source to the large HONO mixing ratios observed at DC. Finally, to evaluate a suspected possible interference of HNO_4 on the HONO mixing ratio measured by the LOPAP, field experiments were conducted by heating sampled air prior to its introduction in the LOPAP device, heating being a convenient way to destroy HNO_4. The selectivity to HNO_4 and the response of the LOPAP during the heating events was also investigated in laboratory by mass spectrometry at Paul Scherrer Institute (PSI).

2. Methods and Site

2.1 HONO measurement method

HONO was measured using a long path absorption photometer (LOPAP) which has been described in detail elsewhere (Heland et al., 2001; Kleffmann et al., 2002). In brief, after being sampled into a temperature controlled stripping coil containing a mixture of sulfanilamide in a 1N HCl solution, HONO is derivatized into a coloured azo dye. The light absorption by the azo dye is measured in a long path absorption tube by a spectrometer at 550 nm using an optical path length of 5 m. The LOPAP did not have long sampling lines or inlet. The stripping coil was placed directly in the atmosphere being sampled. The LOPAP has two stripping coils connected in series to correct interferences. In the first coil (channel 1), HONO is trapped quantitatively together with a small amount of the interfering substances. Assuming that these interfering species are trapped in a similar amount in the second coil (channel 2), the difference between the signals resulting from stripping in each coil provides an interference-free HONO signal (Heland et al., 2001) Air was sampled at a flow rate of 1 L min^{-1} and the flow rate of the stripping solution was of 0.17 mL min^{-1}. Calibrations were performed every five days. Relative deviations of the calibration signal were of 3% and 9% at 3σ for channel 1 and 2, respectively. The quantification limit of the LOPAP instrument used in this study was as low as 1.5 pptv (taken as 10 σ of all zero measurements done by sampling pure N_2) with a time resolution of 9 min. More details on the set up of the LOPAP device in the fields can be found in Kerbrat et al. (2012). Similarly to the first campaign, the amount of

interferences in the second coil was on average 9 ± 7 % of total signal (instead of 10 ± 5 % found by Kerbrat et al. (2012) in 2010/2011). The LOPAP was tested for numerous possible interfering NO_x and NO_y species including alkylnitrates. It was concluded that when significant the two channels approach was able to well correct the HONO data (Kleffmann and Wiesen, 2008). It has, however, to be emphasized that no tests have been conducted for HNO_4.

During the field campaign, HONO was occasionally sampled in the snow interstitial air by pumping air through a PFA tube (5 m long, 4 mm internal diameter) at a flow rate of 1 L min^{-1}. In addition, to evaluate a possible influence of HNO_4 on HONO measurements, field experiments were undertaken by heating air sampled through a 9 m long PFA tube. Tests were performed to evaluate potential loss or formation of HONO in the PFA tubes by running the LOPAP for 30 min with and without a tube connected to the inlet of the LOPAP, sampling air at the same height. In order to account for possible fast natural change of HONO mixing ratios the test was repeated three times successively. The tests were carried out with ambient mixing ratios of 20 pptv as encountered at mid-day December 23rd and 40 pptv in the morning December 28th. In the two cases losses of around 4 pptv and 7 pptv were observed when using the 5 m and 9 m long PFA tube, respectively. These losses will be considered in discussing HONO mixing ratios in interstitial air (see Sect. 3) or the interference of HNO_4 (see Sect. 6).

2.2 Field atmospheric measurements and snow samplings

The second OPALE field campaign took place at DC located over the high East Antarctic plateau from late November 2011 to mid-January 2012. Nitrous acid was measured 1 m above ground level, about 900 m south-southwest from the main Concordia station. Measurements that started December 4th were interrupted from December 9th to 15th, December 16th to 18th, and December 28th to 30th afternoon due to problems on the LOPAP device. January 1st, 2nd, and from January 10th to 13th air measurements were stopped to measure HONO in snow interstitial air. During the measurement campaign, the main wind direction was from the southeast to southwest. Several episodes with wind blowing from North (from 10°W to 60°E sector), i.e. from the direction of the station, were encountered (see the red points in Fig. 1). During some of these pollution events (December 31st around 22:00 for instance), sharp peaks of HONO mixing ratios exceeding 100 pptv were observed. These events were also detected in the NO_x time series (Frey et al., this issue) with sharp peaks in the range of 100 ppbv or more (120 ppbv December 31st around 22:00 for instance).

The ratio of excess of HONO to excess of NO_x during these events is close to 10^{-3}. The ratios of HONO/NO_x reported by measurements made in traffic tunnels range from $3x10^{-3}$ (Kirchstetter et al., 1996) to $8x10^{-3}$ (Kurtenbach et al., 2001). When compared to ratios observed in tunnels, the lower ratio seen in the plume of the DC station when it reaches the sampling line is likely due the rapid photolytic destruction of HONO whose the lifetime is still as short as 20 min at the high solar zenith angles prevailing at DC around 22:00 in summer. In the following the data corresponding to red points reported in Fig. 1 were removed from the HONO data set.

Concurrent measurements of chemical species that are relevant for discussion include ozone, NO, NO_2, OH, and RO_2. Surface ozone was monitored simultaneously to HONO using UV absorption monitors (Thermo electron Corporation model 49I) deployed at DC since 2007 (Legrand et al., 2009). Nitrogen oxides were determined by deploying a 2-channel chemiluminescence detector (Bauguitte et al., 2012; Frey et al., 2013; Frey et al., this issue). The chemiluminescence detector measured NO in one channel and the sum of NO and NO originating from the photolytic conversion of NO_2 in the other channel. As discussed by Frey et al. (2013), among various nitrogen oxides able to interfere on the photolytic conversion channel only HONO has to be considered leading to an overestimation of NO_2 levels by less than 5%. The radicals (OH and RO_2) were measured using chemical ionisation mass spectrometry (Kukui et al., 2012; Kukui et al., this issue). During the campaign the photolysis rate of HONO was documented using a Met-Con 2π spectral radiometer equipped with a CCD detector and a spectral range from 285 to 700 nm (see details in Kukui et al., this issue).

Different surface snow samples were collected at DC and returned to the UK to be used in irradiation experiments (see Sect. 2.3 and Sect. 4). First, the upper 12 cm of snow were collected in December 2010. Second, the upper centimetre of snow corresponding to freshly drifted snow was collected December 6th 2011. The samples were characterized by their specific surface area (SSA). Measurements were performed using an Alpine Snowpack Specific Surface Area Profiler, an instrument similar to that one described by Arnaud et al. (2011) based on the infrared reflectance technique. Briefly, a laser diode at 1310 nm illuminates the snow sample at nadir incidence angle and the reflected hemispherical radiance is measured. The hemispherical reflectance at 1310 nm is related to the SSA using the analytical relationship proposed by Khokanovsky and Zege (2004). The SSA of the drifting snow is close to 26 m^2 kg^{-1}, and the upper 12 cm is 17 m^2 kg^{-1}. Such values appears to be close to typical Dome C values reported in the literature (Gallet et al., 2011), suggesting that

lab experiments conducted on these snow samples (see Sect. 4) may be relevant to discuss at least qualitatively natural processes occurring at DC.

The upper surface snow (from 0 to 1 cm, and from 0 to 12 cm) at DC were also sampled and analysed for major anions and cations following working conditions reported in Legrand et al. (2013). For cations (Na^+, K^+, Mg^{2+}, Ca^{2+}, and NH_4^+), a Dionex 500 chromatograph equipped with a CS12 separator column was used. For anions, a Dionex 600 equipped with an AS11 separator column was run with a quaternary gradient of eluents (H_2O, NaOH at 2.5 and 100 mM, and CH_3OH) allowing the determination of inorganic species (Cl^-, NO_3^-, and SO_4^{2-}) as well as methanesulfonate ($CH_3SO_3^-$). The acidity of samples can be evaluated by the ionic balance between anions and cations with concentrations expressed in micro-equivalents per liter ($\mu Eq\ L^{-1}$):

$$[H^+] = [Cl^-] + [NO_3^-] + [SO_4^{2-}] + [CH_3SO_3^-] - [Na^+] - [K^+] - [Mg^{2+}] - [Ca^{2+}] - [NH_4^+] \quad (1)$$

2.3 Snow irradiation experiments conducted at BAS

As discussed in Sect. 5, model simulations indicate that the production of HONO from the reaction of OH with NO is far too weak to explain observations at Dome C and that an additional light driven HONO source is needed. To quantify a possible photochemical snow source of HONO, lab experiments were conducted at BAS by irradiating snow collected at DC and measuring gas-phase evolution of NO and NO_2 with a 2-channel chemiluminescence detector (Bauguitte et al., 2012) as deployed at DC (Frey et al. 2013, Frey et al. this issue) and HONO with the LOPAP that ran at DC during the 2010/2011 and 2011/2012 campaigns. A 20 cm long cylinder (6 cm inner diameter) was filled with ~ 120 g of snow inside an airtight glass reaction chamber (total length of 40 cm, 6 cm inner diameter) and put in a freezer of which the temperature was varied between -5 to -35°C. Further details on the characteristics of the reaction chamber can be found in Meusinger et al. (2014). The reaction chamber is maintained vertically in a freezer and a 1000 W Xenon-arc lamp was put above the freezer. The snow was irradiated by directing the light axially along the tube through a quartz window, which makes up the top surface of the chamber. Chemically pure air was supplied to the chamber from a pure air generator (Ecophysics, PAG003) in which air is dried at -15°C. To match the relative humidity of the snow under investigation and limit metamorphism the chemically pure (humid) air dry was passed through a cold trap at the temperature of the experiment. Note that with this system and for temperatures above -30°C, no condensation trace was observed in the tubes outflow of the chamber. The flow rate of zero air was 4.3 L min^{-1} while the detection systems sampled processed air at a rate of 2.0 L min^{-1} for NO_x and

1.0 L min^{-1} for HONO. The overflow of 1.3 L min^{-1} was diverted through a flow metre to check for potential leaks. While the inlet line between the reaction chamber and the NO_x analyser was several m long, the length between the outlet of the reaction chamber and the LOPAP inlet was kept as short as possible (i.e. 25 cm). To do so the inlet of the LOPAP was arranged in the freezer. The wavelength range of the 1000 W Xenon-arc lamp (Oriel Instruments) was 200-2500 nm, modulated using filters with various cut-on points. The short residence time of NO_2 (~ 4 s) in our small chamber prevents significant photolysis of NO_2 to occur during the experiments. Indeed, the J_{NO2} of 2 10^{-2} s^{-1} measured by Cotter et al. (2003) for a 1000 W Xenon-arc lamp, as also used in the present study, leads to a lifetime of NO_2 with respect to photolysis of 50 s at the front of the snow block.

2.4 Experiments performed at PSI to investigate a possible HNO_4 interference on HONO measurements

As will be discussed in Sect. 6, it may be difficult to reconcile typical mixing ratios of HONO measured 1 m above surface snow at Concordia with a reasonable estimate of the mixing ratio of HONO owing to emissions from snow due to snowpack photochemistry. It was suspected that HNO_4 was detected and measured as HONO by the LOPAP instrument. As briefly reported below, a few experiments conducted at PSI indicate that the LOPAP instrument does have an interference for HNO_4. Mixing ratios of HNO_4 were not measured at DC, so the aim of the experiments described below was not to quantify the interference to enable correction of the Concordia HONO data, but to demonstrate that such an interference exits. The result of an experiment conducted under specific conditions is reported. A full characterization of the interference on HONO at various mixing ratios of HNO_4 in the presence or not of other trace gases present at DC is beyond the scope of this paper.

The interference of the LOPAP device was examined at the PSI where a gas-phase synthesis of HNO_4 has been developed by irradiating a mixture of $NO_2/H_2O/CO/O_2/N_2$ at 172 nm (Bartels-Rausch et al., 2011). By-products of the synthesis are HONO, HNO_3, and H_2O_2. The synthesis gas was fed into the sampling unit of the LOPAP and the resulting LOPAP signals in presence and absence of HNO_4 were compared. Heating the synthesis gas to a temperature of 100°C prior to sampling by the LOPAP allowed selective removal of HNO_4 from the gas mixture. The mixing ratios of HONO, NO_2, H_2O_2 and O_3 that are present in the synthesis gas were independently monitored with a chemical ionisation mass spectrometer (CIMS), which was calibrated by using several analysers as detailed in Ulrich et al. (2012). An example of the mixing ratios of HNO_4 and HONO measured by CIMS and of the

corresponding LOPAP signals in channel 1 and 2 is shown in Fig. 2. The relative amount of HONO (780 pptv) and HNO_4 (1000 pptv) observed in the synthetized mixture (prior heating) is typical for this synthesis (Bartels-Rausch et al., 2011). The experiment shows the response of the signals when the heating trap used to decompose HNO_4 is applied. As seen in Fig. 2, the mixing ratios of HONO, NO_2, H_2O_2 or O_3 that may influence the response of the LOPAP instrument did not change upon the thermal decomposition of HNO_4. A decrease of the LOPAP signal in channel 1 is observed during the heating event, indicating that 1 ppbv of HNO_4 corresponds to a signal in the LOPAP of 150 pptv. Examination of the signals of the two LOPAP channels (Fig. 2) suggests that HNO_4 has been efficiently sampled in the first channel. It is well known that HNO_4 efficiently decomposes to NO_2^- in acidic solutions (Regimbal and Mozurkewich, 1997), just like HONO does in the LOPAP sample unit. Based on the identical hydrolysis products, one might thus expect a rather large interference. The high sampling efficiency of HONO and potentially HNO_4, both of which have similar partitioning coefficients to acidic solutions, is driven by the fast reaction of their hydrolysis product (NO_2^-) with the reagents in the sampling solution of the LOPAP instrument. A full characterization of the interference by HNO_4 (its behaviour and quantification over a large range of concentrations, in the presence or absence of other gases) is needed to improve the use of the LOPAP in very cold atmospheres. We suggest a detailed investigation of LOPAP instrument response to different compositions of test gas mixture (i.e. with larger mixing ratios of H_2O_2), and with an investigation of the potentially complex (non-linear) chemistry of sampled gases. At this stage we can only exclude an oxidation of the dye used in the LOPAP instrument by HNO_4, as careful inspection of the absorption spectrum of the LOPAP dye reveals no significant change during heating. Assuming the interference of HONO signal by HNO_4 to be linear, one would expect an interference of ~15 pptv in the HONO signal due to a mixing ratio of 100 pptv of HNO_4. Given the absence of measurements of the mixing ratio of HNO_4 at Concordia, further experiments were conducted in the field at Concordia to directly estimate this interference as detailed in Sect. 6.

3. HONO observations at Concordia

Removing data suspected to have been impacted by pollution from station activities (see Sect. 2.2), one-minute average mixing ratio of 35 ± 14 pptv is observed in December 2011/January 2012 compared to 28 ± 12 pptv measured by Kerbrat et al. (2012) for December 2010/ January 2011/2012.

The mean diurnal cycles of surface ozone, HONO, air temperature and the PBL height simulated by MAR are reported and compared for the two summers in Fig. 3. In polar region, the strong static stability of the atmosphere often inhibits vertical mixing of surface emissions between the surface boundary layer and the rest of the atmosphere. At DC, the surface absorbs solar radiations during the day, heats the lower atmosphere and generates positive buoyancy that is responsible for an increase of turbulent kinetic energy and the subsequent increase of the boundary layer height seen in Fig. 3. This boundary layer is referred to as the "daytime boundary layer". The surface cooling after 17:00 generates negative buoyancy near the surface. A new boundary layer referred as the “night-time boundary layer” develops but remains less active than the previous daytime boundary layer. The collapse of the boundary layer after 17:00 seen in Fig. 3 is in fact the representation of the transition between the daytime and nighttime boundary layer.

The two mean summer ozone records indicate a drop of 1 to 2 ppbv around mid-day compared to early morning and evening values (Fig. 3). This small surface ozone change over the course of the day at DC has already been observed by Legrand et al. (2009) who attributed it to the increase of the PBL height in the afternoon that counteracts a local photochemical production of O_3 in the range of 0.2 ppbv hr^{-1} during day-time.

Consistently with the previous 2010/2011 measurements from Kerbrat et al. (2012), the HONO mixing ratios exhibit a well-marked diurnal variation characterized by morning (around 5:00-7:00) and evening (around 20:00) maxima exceeding mid-day values by some 10 pptv. Therefore, in addition to an expected more efficient photolysis of HONO during the day, the increase of the daytime boundary layer may also accounts for the observed decreased HONO mixing ratios during the day in spite of a more active snow source (see discussions in Sect. 5). Such a diurnal variability characterized by noon minimum was also observed for NO_x by Frey et al. (2013) and attributed to the interplay between photochemical snow source and boundary layer dynamics.

As shown in Fig. 3, the larger HONO mixing ratios calculated for 2011/2012 (diurnal mean of 35 ± 5.0 pptv) with respect to the 2010/2011 ones (diurnal mean of 30.5 ± 3.5 pptv) concern both the mid-day minimum and the morning/evening maxima. The difference between the two summers is however reduced when the first week of measurements undertaken December in 2011 is removed with a lower diurnal mean (31.7 ± 4.3 pptv instead of 35 ± 5 pptv over the entire measurement period, see the blue points in Fig. 3). The case of beginning of December 2011 with respect to the rest of the summer 2011/2012 is highlighted in Fig. 3. It can be seen that the far thinner PBL height of early December (maximum of 145

m instead of 350 m over the entire period) may have lead to a more confined HONO production (see violet points in Fig. 3). Note also the relatively high ozone mixing ratios at that time (33 ± 4 ppbv in early December instead of 26 ± 1 ppbv over the entire period). Conversely, at the end of the period the PBL became thicker (maximum of 570 m) and the mixing ratios of ozone (24 ± 1 ppbv) and nitrous acid (31 ± 4 pptv) were lower than on average (see red points in Fig. 3). Finally, early December 2011 the highest daily average mixing ratio of HONO was observed December 7th and 8th (56 pptv, Fig. 1) correspond not only to a thin PBL but also to lowest value of total ozone column (260 DU instead of 296 ± 20 DDU on average) measured by the SAOZ at DC. Similarly, during the 2010/2011 campaign the highest values reported at the end of the campaign (44 pptv from 15th to 18th January) by Kerbrat et al. (2012) correspond to the lowest value of total ozone column (270 DU instead of 303 ± 17 DDU on average). It therefore seems that HONO mixing ratios measured at 1 m at DC are also sensitive to the UV actinic flux reaching the surface. This link between stratospheric ozone and photochemistry of snow at the ground is discussed in more detail by Frey et al. (this issue).

It therefore seems that one of the main causes for the difference between the 2011/2012 and 2010/2011 mean summer values is mainly related to the slightly different atmospheric vertical stability conditions experienced over the different sampling times of the two summers, with an earlier HONO sampling in December 2011 than in December 2010 leading to higher HONO mixing ratios in a very thin and stable boundary layer. In conclusion, this second study of HONO confirms the abundance of this species in the lower atmosphere at DC with a typical mean mixing ratio of 30 pptv from mid-December to mid-January.

As already discussed by Kerbrat et al. (2012) (see also Sect. 5), the existence of a large photochemical source of HONO in the snow-pack is needed to explain these large mixing ratios of HONO measured above the snowpack. Measurements of the mixing ratio of HONO were therefore performed in snow interstitial air at different depths. From the top few cm of the snowpack down to 75 cm depth, mixing ratios of HONO in snowpack interstitial air tended to exceed those in the air above the snowpack, supporting the existence of a snow source of HONO (Fig. 4). However, given the interference of HNO_4 on HONO mixing ratio data as discussed in Sect. 6, it is difficult to use the observed vertical gradient of HONO mixing ratio to derive an estimate of emission of HONO from the snowpack. Indeed, typical values of HNO_4 mixing ratios are available in lower atmosphere of the Antarctic plateau (Sect. 6) but not yet in snow interstitial air. Also it remains difficult to accurately estimate the

production rate of HNO_4 in snow interstitial air from the reaction of NO_2 with HO_2 versus its uptake on natural ice surface.

To confirm the snowpack as a source of HONO (and as detailed in the following section) we carried out a laboratory experiment to evaluate the ratio of HONO to NO_x released from natural surface snows collected at DC under controlled laboratory conditions (i.e. wavelength of light, temperature, snow specific area) to estimate the HONO snow emission flux relative to the snow emission flux of NO_x for the same snowpack as derived from atmospheric concentration vertical gradient measured during the campaign by Frey et al. (this issue).

4. Lab experiments on natural snow collected at DC

Table 1 summarized the results of experiments conducted at BAS by irradiating surface snows collected at Dome C (see Sect. 2.3). NO_x and HONO are produced when snow is irradiated. Several laboratory experiments were conducted to investigate the wavelength, temperature and snow chemical composition dependence of HONO release from snow. Similar to previous laboratory experiments conducted by Cotter et al. (2003) on surface snows collected in coastal Antarctica, the NO_x release is found to halve when the optical filter in the front of the irradiation lamp (cut off for < 295 nm) is replaced by a cut off filter for illumination wavelength smaller than 320 nm (Table 1). Cotter et al. (2003) demonstrated no measurable emission of NO_x from the snow when illuminated with a lamp with wavelengths shaded below 345 nm, being consistent with NO_3^- photolysis. Fig. 5 illustrates the wavelength dependence of HONO release showing the effect of insertion of a filter with different cut-on points. Similarly to the NO_x, the HONO release is decreased by a factor two when inserting the filter at 320 nm and become insignificant at 385 nm (Table 1).

While the observed wavelength dependency of the NO_x release supports the hypothesis that the photolysis of nitrate present in snow is the major source of released NOx (via its major channel: $NO_3^- + h\nu \rightarrow NO_2 + O^-$), for HONO it is still unclear if either the nitrate photolysis efficiently produces directly HONO from hydrolysis of NO_2^- produced by the second channel of the nitrate photolysis ($NO_3^- + h\nu \rightarrow NO_2^- + O$) or HONO is secondary produced from NO_2 (Villena et al., 2011). Indeed, lab experiments conducted on nitrate doped ice suggest that the first channel is a factor of 8-9 more efficient than the second one. It is suspected that the HONO production may be significantly higher than it is when considering this second channel since the NO_2 produced by the first channel may subsequently act as a precursor of HONO. The wavelength dependency of HONO release observed during previous

experiments does not however help to separate the primary and secondary source of HONO during irradiation since they were done with chemically pure air and when placing the cut off filter at 385 nm we suppress the primary source of HONO as well as NO_2 that is needed for secondary HONO production.

Among possible secondary productions it is generally accepted that the reduction of NO_2 on photo-sensitized organic material like humic acid (George et al., 2005; Bartels-Rausch et al., 2010) would proceed more efficiently than the disproportionation reaction of NO_2 ($2\ NO_2 + H_2O \rightarrow HONO + HNO_3$) (Finlayson-Pitts et al., 2003). As discussed by Grannas et al. (2007), the relevance of this secondary production was supported even for Antarctica by the significant presence of dissolved fulvic acid reported for Antarctic snow (26-46 ppbC) by Calace et al. (2005). However, the previously assumed ubiquitous presence of organics in polar snow that is needed to reduce NO_2 into HONO was recently reviewed by Legrand et al. (2013) who found that organics (and humic acids) are far less abundant in Antarctica compared to Greenland or mid-latitude glaciers like the Alps. For instance, the typical dissolved organic content of summer surface snow is only 10-27 ppbC at Concordia (Legrand et al., 2013) against 110 ± 45 ppbC at Summit and 300 ppbC in the Alps. Furthermore, recent HULIS measurements of surface snows collected at DC do not confirm the previously observed abundance (2 ppbC instead of 26-46 ppbC). From lab experiments conducted by irradiating ice films containing humic acid in the presence of NO_2, Bartels-Rausch et al. (2010) derived production rates of HONO from NO_2. From that the authors roughly estimated light driven HONO fluxes of 10^{13} molecule m^{-2} s^{-1} from snow covered surface area assuming the presence of 100 pptv NO_2 in the snow interstitial air and a concentration of 10 ppbC of humic acid in snow. Keeping in mind uncertainties in extrapolating lab experiments to conditions relevant to the lower atmosphere at Dome C, with typical NO_2 mixing ratios of 1 to 10 ppbv in interstitial air at 10 cm below the surface at Dome C (Frey et al., this issue), the presence of 2 ppbC of HULIS in snow may still lead to a significant HONO production from NO_2 at the site. If HULIS are located at the surface of snow grains, much more than 2 ppbC of HULIS would be available to react with NO_2 present in interstitial air of the snowpack to produce HONO.

Irradiation experiments with insertion of the filter at 295 nm were conducted at temperatures ranging from 240 to 260 K. As seen in Table 1, whereas the NO_x release was found to be temperature independent (as previously shown by Cotter et al., 2003), a large dependence is found for HONO with an increase by a factor of 2.2 when the temperature of snow is increased from 240 to 260 K. A temperature dependence of the HONO emissions is

expected since the partition coefficient of HONO between ice and air increases by a factor of 5.8 between 240 K and 260 K (Crowley et al., 2010). As a consequence the HONO to NOx release is smaller at 240K than at 260K. For the example of the surface snow reported in Table 1, this ratio steadily increases from 0.3 at 240 K, 0.5 at 250 K to 0.8 at 260 K.

As reported in Table 1, experiments were made with DC snow containing from 160 to 1400 ppb of nitrate. As expected higher nitrate content leads to higher snow release of NO_x and HONO but the increase of HONO is larger than the one of NO_x. For instance, at a temperature close to -20°C, the first upper cm of surface snow releases almost twice more HONO compared NO_x than the snow collected from the surface to 12 cm depth. The more acidic character of the snow collected in the upper first centimetre compared to the one collected down to 12 cm below the surface (see Table 1) may favour the release of a weak acid species like HONO.

5. Model calculations

Observed atmospheric mixing ratios were compared with steady-state calculations made by considering major gas-phase sources and sinks of HONO. The major sink of HONO is its photolysis. The photolysis rate constant (J_{HONO}) were measured with a 2π spectroradiometer (see Sect. 2.2). The value of J_{HONO} was calculated for light from 4π steradians from the downwelling value of J_{HONO} measured over 2π steradians by assuming a surface albedo of 0.95, a typical value for regions covered by dry snow and wavelength shorter than 400 nm (Hudson et al., 2006; France et al., 2011). The main gas-phase production of HONO is the reaction of NO with OH radicals. Steady-state calculations indicate that under noon conditions encountered at DC (a J_{HONO} value of 3.7×10^{-3} s^{-1}, 5×10^6 OH rad. cm^{-3} (Kukui et al., this issue), and 50 pptv of NO (Frey et al., this issue)), a HONO mixing ratio of 1 pptv is expected. Steady-state calculated diurnal HONO profile (Fig. 6) suggests a HONO maximum of 2.5 pptv at 19:00 due to the presence of a maximum of 120 pptv of NO (Frey et al., this issue).

Another gas-phase source of HONO was recently proposed by Li et al. (2014) via reaction of $HO_2(H_2O)$ complex with NO_2:

$$HO_2 + NO_2 \rightarrow HO_2NO_2 \quad (2)$$

$$HO_2 + H_2O \leftrightarrow HO_2(H_2O) \quad (3)$$

$$HO_2(H_2O) + NO_2 \rightarrow HONO + \text{other products} \quad (4)$$

Reaction of $HO_2(H_2O)$ complex with NO_2 was first suggested by Sander and Peterson (1984) to explain the observation of a linear dependence of the effective rate constant of the reaction of HO_2 with NO_2 on the concentration of water vapour in the temperature range 275-298 K. Assuming reaction mechanism (2-4) Sander and Peterson (1984) derived temperature dependence for the effective third-order rate constant of the reaction $HO_2+NO_2+H_2O$, $k^{III}_4(T)$, with $k^{III}_4(T)$ representing the product $k_4 \times K_3$, where k_4 is the bimolecular rate constant for reaction $HO_2(H_2O)$ with NO_2 and K_3 is equilibrium constant for reaction (3). The possible contribution of reaction (4) to form HONO at Concordia was evaluated by assuming a unity yield of HONO for the reaction (4). The rate constant $k_4(T)$ in the temperature range 275-298 K was estimated from the $k^{III}_4(T)$ data of Sander and Peterson (1984) using recent recommendations for $K_3(T)$ and $k_2(T)$ from Sander et al. (2011): $k_4(T) = k^{III}_4(T) / K_3(T) \times k_2(T) / k_2(T)^{Sander}$, where $k_2(T)^{Sander}$ are data from Sander and Peterson (1984). The values of $k_4(T)$ at low temperatures encountered at Concordia were obtained by extrapolating the $k_4(T)/k_2(T)$ data from Sander and Peterson (1984) and assuming a logarithmic dependence of $k_4(T)/k_2(T)$ on 1/T, similar to reaction of $HO_2(H_2O)$ with HO_2 (Sanders et al., 2011). The resulting dependence ($k_4(T)/k_2(T) = 10^{-1505.3/T(K)+5.4}$) predicts significantly lower water enhancement effect at low temperature (k_4/k_2=0.12 at 240K compared to 2.2 at 298K). Using these k_4 values and observations of OH, NO, HO_2, NO_2 and H_2O, the low temperatures encountered at Concordia make negligible the formation of HONO from the reaction (4). This hypothetical HONO source would contribute for 10-20% of the HONO production from the reaction OH+NO and would result in less than 1% of the measured HONO.

An additional source of HONO is obviously required to account for observed mixing ratios of a few tens of pptv. On the basis of laboratory experiments presented in Sect. 4, we examine to what extent the snow photochemical source of HONO accounts for atmospheric observations of HONO at Concordia. Simulations were made with a numerical 1-D box model that considers, in addition to the above-mentioned gas-phase sources and sinks of HONO, a flux from the snow and its diffusive vertical transport. The turbulent diffusion coefficients (K_z) were calculated by the regional atmospheric MAR model (Modèle Atmosphérique Régional). Since cloud cover is responsible for an increase of around 50% of the down-welling long-wave radiations in summer at DC, when the cloud cover is underestimated, the surface heat budget is not well simulated and this strongly impacts the turbulence simulated by the model. We therefore performed calculations only for days with clear sky conditions (see Fig. 1).

We used the MAR model with a horizontal resolution of 20 km centred at Concordia; a top level is at 1 hPa with 100 vertical levels. The vertical resolution is 0.9 m up to 23 m above the surface, and decreases upward. MAR K_z values are linearly interpolated to the vertical grid used in our 1D simulation, spacing 0.1 m from the ground to 5 m, 0.2 m from 5 to 7 m, 0.5 m from 7 to 10 m, around 1 m from 10 to 20 m and then increases up to 120 m at 1200 m height, respectively. MAR data above a height of 1200 m were not used here since during investigated period the top of the PBL remained below this value. The MAR model uses primitive equations with the hydrostatic assumption. A description of the model that has been validated with respect to observations from Automatic Weather Station at DC, is given by *Gallée and Gorodetskaya* [2008] and references therein. Parametrization of turbulence in the lowest model layer of MAR is based on the Monin-Obukhov Similarity theory (MOST). Above the surface boundary layer, turbulence is parametrized using the E - ε model that includes two prognostic equations for turbulent kinetic energy and its dissipation. MAR simulations have been recently validated for winter with respect to observations from Automatic Weather Station at Concordia (G*allée and Gorodetskaya*, 2008) and for summer (*Gallée et al*., this issue). The boundary layer (PBL) height was computed from MAR simulations by taking the height where the turbulent kinetic energy decreases below 5 % of the value of the lowest layer of the model.

In Fig. 6 we report the simulated diurnal cycle of HONO mixing ratio at 1 m above the ground at Concordia when a photochemical snow release of HONO is applied. The HONO flux used in these calculations was obtained by multiplying the values of the NO_x snow emission flux derived from field observations at Concordia (Frey et al., this issue) by the temperature dependent factor reported for surface snow in Table 1. Since, as discussed in section 4, lab experiments indicate no significant change of the ratio of HONO/NOx release when replacing the filter with a 295 nm cut-on point by the one at 320 nm (Table 1), and given a maximum of the aqueous absorption cross section for nitrate centered at 300 nm (Gaffney et al., 1992), we have assumed that the ratio is similar under the two wavelength conditions and used the temperature dependency found when the filter with a cut-off point at 295 nm was inserted (Table 1). In this way under temperature conditions encountered at Dome C we have assumed a $HONO/NO_x$ ratio ranging from 0.57 during the day (at -25°C) and 0.3 at night (at -35°C). The derived HONO snow emission flux estimate would represent an upper limit since, as seen in Sect. 4, the upper 12 cm of snow emits less HONO than NO_x compared to the surface snow. As seen in Fig. 6, using this upper estimate of the HONO snow emission (mean diurnal value of 0.8×10^9 molecules cm^{-2} s^{-1}) simulations show that, in

addition to around 1.2 pptv of HONO produced by the NO oxidation, the HONO snow emissions can account for 10.5 pptv of HONO in the atmosphere at Concordia. Assuming a lower HONO to NO_x ratio of snow emissions as suggested by the experiment conducted with the upper 12 cm of snow collected at Concordia (Table 1), mean diurnal HONO emission of $0.5x10^9$ molecules cm^{-2} s^{-1} is estimated leading to a related HONO mixing ratio of 6.5 pptv (total of 8 pptv together with NO oxidation). It has also to be emphasized that these estimated HONO snow emission fluxes were derived from values of the $HONO/NO_x$ photochemical production ratio observed in laboratory experiments carried out by flowing zero air through the snow instead of natural interstitial air of which the chemical composition may be very different.

An upper value of the ratio of HONO to NO_x mixing ratios often serves as a reference value to discuss the consistency of HONO mixing ratios (Kleffmann and Wiesen, 2008; Villena et al., 2011). Steady-state calculations indicate that the $HONO/NO_x$ ratio reaches a maximum value equal to the ratio of HONO to NO_x lifetimes (τ_{HONO}/τ_{NOx}), when it is assumed that HONO is the sole source of NO_x. The measured HONO photolysis rate constants (see Sect. 2.2) indicate an atmospheric lifetime of HONO at Concordia ranging from 4.5 min to 24 min at 12:00 and 0:00, respectively. Using OH and HO_2 concentrations observed by Kukui et al. (this issue), an atmospheric lifetime of NO_x ranging from 3 hours at 12:00 to 7 hours at 0:00 can be estimated. From that, the upper limit of the $HONO/NO_x$ ratio at Concordia would be close to 0.03 and 0.06 at 12:00 and 0:00, respectively. Using the HONO mixing ratios simulated when a mean diurnal HONO snow emission of $0.8x10^9$ molecules cm^{-2} s^{-1} is considered (Fig. 6) and NO_x mixing ratios observed at Concordia (around 200 pptv, Frey et al., this issue), we calculate a mean diurnal $HONO/NO_x$ ratio of 0.06. This value slightly exceeds the maximum steady state $HONO/NO_x$ ratio estimated from HONO and NO_x photochemical lifetimes. Note, however, that more accurate estimation of the upper limit of the $HONO/NO_x$ ratio should take into account also HONO and NO_x vertical distributions determined by the vertical diffusivity and the conversion of HONO to NO_x, as well as by a possibility of non steady state conditions. As the consideration of these factors may lead to a higher $HONO/NO_x$ ratio, the higher $HONO/NO_x$ ratio of about 0.06 cannot be considered as a strong indication of an error in the simulated HONO mixing ratios derived with an assumed HONO snow emission of $0.8x10^9$ molecules cm^{-2} s^{-1}.

6. A possible HNO_4 interference on HONO measurements made with a LOPAP ?

As discussed in the previous section, field measurements of boundary layer HONO mixing ratios at DC in summer (30 pptv) significantly exceed values calculated by considering a HONO snow source estimated from the observed NO_x snow source and the relative abundance of HONO and NO_x releases observed during snow irradiation BAS experiments (8 to 12 pptv). As reported in Sect. 2.4, lab experiments conducted with the LOPAP have shown a possible overestimation of HONO by ~15 pptv due to the presence of 100 pptv of HNO_4.

Although HNO_4 data are not available at Dome C, its presence is very likely since its atmospheric lifetime with respect to thermal decomposition becomes significant at low temperatures (lifetime close to 2 h at -20°C, Sanders et al., 2011). Whereas the first measurements of HNO_4 in Antarctica reported moderate mixing ratios (mean of 25 pptv observed over a few days in December 2000 at the South Pole, Slusher et al., 2002), following investigations revealed higher values. First, from 40 pptv in December to 60 pptv during the second half of November were observed in 2003 at the South Pole (Eisele et al., 2008). Second, a mean value of 64 pptv (up to 150 pptv) was observed between the ground and 50 m elevation over the Antarctic plateau (Slusher et al. 2010). These latter values of HNO_4 mixing ratio together with the above-discussed inconsistencies between simulations and observations stimulate efforts to investigate a possible interference of HNO_4 on the LOPAP instrument. Note that given the HNO_4 lifetime with respect to thermal decomposition of a few hours at -20°C, we don't expect interference during snow experiments conducted at BAS since HNO_4 initially present in snow collected at DC would have been destroyed during its storage of a few months at -20°C. Furthermore, production of HNO_4 during the BAS experiments (Sect. 4) following the release of NO_2 under irradiation of snow is far too slow to have significantly impacted HONO measurements.

Even though laboratory experiences conducted at PSI under certain conditions clearly showed that the LOPAP instrument has interference for HNO_4 (see Sect. 2.4), the absence of HNO_4 atmospheric data at Dome C hampers any accurate attempt to correct HONO data from the presence of HNO_4. Instead, field experiments were conducted at Concordia heating the air sampled by the LOPAP to thermally decompose HNO_4. This air was heated by sucking air through a 8 m long PFA tube covered with a temperature controlled heating tape and placed in an insulated box. When heating the tube, the air temperature in the PFA tube was of 37°C leading to a lifetime of HNO_4 with respect to its thermal decomposition of 3.2 s (Sanders et al., 2011). The experiment was performed by running the LOPAP for ~ 20 min with and without heating the tube connected to the inlet of the LOPAP. In order to account for possible

fast natural change of HONO mixing ratios the test was repeated three times successively. A systematic drop of HONO values was observed. Given the applied air sampling flow rate of 1.78 L min^{-1} (1 L STP min^{-1}), the residence time of the air in the tube is 3.3 s. If attributed to the thermal decomposition of HNO_4 during the heating (64% under these working conditions), the mean observed drop of 5.5 pptv of HONO would correspond to an HNO_4 artefact of around 9 pptv.

This indirect estimation of an overestimation of HONO measurements due to the presence of HNO_4 is consistent with experiences conducted at PSI if the presence of 50-100 pptv of HNO_4 is assumed at Dome C. On the other hand, the difference between observed and simulated HONO mixing ratios presented in Sect. 5 suggests a mean diurnal overestimation close to 20 pptv (ranging from 17 pptv around noon to 22 pptv during the night). In their discussions of the observed levels of HO_x radicals, Kukui et al., (this issue) found that the consideration of 30 pptv of HONO is inconsistent with radical observations leading to about 2 times overestimation of RO_2 and OH concentrations. Conversely, neglecting the OH production from HONO leads to an underestimation of radical levels by a factor of 2. Kukui et al. (this issue) showed that a quite fair agreement with OH measurements is achieved with HONO mixing ratios derived from the 1D modelling with a HONO snow emission flux equal to about 30% of that of NO_x. Finally, though being slightly higher, the best guess of HONO mixing ratios derived in Sect. 5 for Concordia (8 to 12 pptv) are in the range of mixing ratios measurements made at the South Pole using laser-induced fluorescence (6 pptv, Liao et al., 2006).

7. Conclusions

This second study of HONO conducted in the atmosphere of the East Antarctic plateau by deploying a LOPAP confirms unexpectedly high mixing ratios close to 30 pptv. A mixing ratio of 8-12 pptv can be rationalized based on emissions of HONO from snow of 0.5-0.8x10^9 molecules cm^{-2} s^{-1} derived from studies of the irradiation experiments surface snow collected from Concordia and scaled down to the NO_x emissions derived from observations made at DC by Frey et al. (this issue). Experiments conducted in the field and in the lab to identify the cause of such a discrepancy point to a possible overestimation of HONO in the range of 10 to 20 pptv due to the important presence of HNO_4 in this cold atmosphere. An accurate correction of the HONO data from the presence of HNO_4 is not yet possible. Further work, both in the lab to quantify the interference at different levels of HNO_4 and in the presence of

various other species and in the field at Concordia to obtain mixing ratios of HONO and HNO_4 at the same time are needed.

Acknowledgements. The OPALE project was funded by the ANR (Agence National de Recherche) contract ANR-09-BLAN-0226. The measurement of the specific snow area was developed in the framework of the MONISNOW projet funded by the ANR-11-JS56-005-01contract. National financial support and field logistic supplies for the summer campaign were provided by Institut Polaire Français-Paul Emile Victor (IPEV) within programs N° 414, 903, and 1011. M.D. King was supported by NERC NE/F0004796/1 and NE/F010788, NERC FSF grants 555.0608 and 584.0609. Thanks to our Italian colleagues from Meteo-Climatological Observatory of PNRA for the meteorological data collected at Dome C.

References:

Arnaud, L., Picard, G., Champollion, N., Dominé, F., Gallet, J.C., Lefebvre, E., Fily, M., and Barnola, J.M.: Measurement of vertical profiles of snow specific surface area with a 1 cm resolution using infrared reflectance: instrument description and validation, J. of Glaciol., 57 (201), 17–29, 2011.

Bartels-Rausch, T., Brigante, M., Elshorbany, Y.F., Ammann, M., D'Anna, B., George, C., Stemmler, K., Ndour, M., and Kleffmann, J. : Humic acid in ice: Photo-enhanced conversion of nitrogen dioxide into nitrous acid, Atmos. Environ., 44, 5443–5450, doi:10.1016/j. atmosenv.2009.12.025, 2010.

Bartels-Rausch, T., Ulrich, T., Huthwelker, T., and Ammann, M.: A novel synthesis of the radiactively labelled atmospheric trace gas peroxynitric acid, Radiochim. Acta, 99, 1–8, doi:10.1524/ract.2011.1830, 2011.

Bauguitte, S.J.-B., Bloss, W.J., Evans, M.J., Salmon, R.A., Anderson, P.S., Jones, A.E., Lee, J.D., Saiz-Lopez, A., Roscoe, H.K., Wolff, E.W., and Plane, J.M.C.: Summertime NOx measurements during the CHABLIS campaign: can source and sink estimates unravel observed diurnal cycles?, Atmos. Chem. Phys., 12(2), 989–1002, doi:10.5194/acp-12-989-2012, 2012.

Beine, H.J., Amoroso, A., Dominé, F., King, M., Nardino, M., Ianniello, A., and France, J. L.: Surprisingly small HONO emissions from snow surfaces at Browning Pass, Antarctica, Atmos. Chem. Phys., 6, 2569–2580, http://www.atmos-chem-phys.net/6/2569/2006/, 2006.

Calace, N., Cantafora, E., Mirante, S., Petronio, B. M., and Pietroletti, M.: Transport and modification of humic substances present in Antarctic snow and ancient ice, J. Environ. Monit., 7, 1320-1325, 2005.

Chan, W.H., Nordstrom, R.J., Galvert, J.G., and Shaw, J.H.: An IRFTS spectroscopic study of the kinetics and the mechanism of the reactions in the gaseous system, HONO, NO, NO_2, H_2O, Chem. Phys. Lett., 37(3), 441–446, doi:10.1016/0009-2614(76)85010-5, 1976.

Chen, G., Davis, D., Crawford, J., Nowak, J.B., Eisele, F., Mauldin, R.L., Tanner, D., Buhr, M., Shetter, R., Lefer, B., Arimoto, R., Hogan, A., Blake, D.: An investigation of South Pole HOx chemistry: comparison of model results with ISCAT observations, Geophys. Res. Lett., 28 (19), 3633-3636, 2001.

Chen, G., Davis, D., Crawford, J., Mauldin III, R., Eisele, F., Huey, G., Slusher, D., Tanner, D., Dibb, J., Buhr, M., Hutterli, M., McConnell, J., Lefer, B., Shetter, R., Blake, D., Lombardi, K., and Arnoldy, J. : A reassessment of HOx South Pole chemistry based on observations recorded during ISCAT 2000, Atmos. Environ., 38(32), 5451–5461, doi:10.1016/j.atmosenv.2003.07.018, 2004.

Cotter, E.S.N., Jones, A.E., Wolff, E.W., and Bauguitte, S.J.-B.: What controls photochemical NO and NO_2 production from Antarctic snow? Laboratory investigation assessing the wavelength and temperature dependence, J. Geophys. Res., 108(D4), 4147, doi:10.1029/2002JD002602, 2003.

Crowley, J.N., Ammann, M., Cox, R.A., Hynes, R.G., Jenkin, M.E., Mellouki, A., Rossi, M.J., Troe, J., and Wallington, T.J. : Evaluated kinetic and photochemical data for atmospheric chemistry: Volume V – heterogeneous reactions on solid substrates, Atmos. Chem. Phys., 10(18), 9059–9223. doi:10.5194/acp-10-9059-2010, 2010.

Davis, D., Nowak, J.B., Chen, G., Buhr, M., Arimoto, R., Hogan, A., Eisele, F., Mauldin, L., Tanner, D., Shetter, R., Lefer, B., and McMurry, P. : Unexpected high levels of NO observed at South Pole, Geophys. Res. Lett., 28(19), 3625–3628, doi:10.1029/ 2000GL012584, 2001.

Dibb, J.E., Arsenault, M., Peterson, M.C., and Honrath, R.E. : Fast nitrogen oxide photochemistry in Summit, Greenland snow, Atmos. Environ., 36, 2501-2511, doi:10.1016/S1352-2310(02)00130-9, 2002.

Dibb, J.E., Huey, L.G., Slusher, D.L., and Tanner, D. J.: Soluble reactive nitrogen oxides at South Pole during ISCAT 2000, Atmos. Environ., 38, 5399–5409, 2004.

Eisele, F., Davis, D.D., Helmig, D., Oltmans, S.J., Neff, W., Huey, G., Tanner, Chen, G., Crawford, J ., Arimoto, R., Buhr, M., J., Mauldin, L., Hutterli, M., Dibb, J., Blake, D., Brooks, S.B., Johnson, B., Roberts, J.M., Wang, Y., Tan, D., and Flocke, F. : Antarctic tropospheric chemistry investigation (ANTCI) 2003 overview, Atmos. Environ., 42(12), 2749–2761, doi:10.1016/j.atmosenv.2007.04.013, 2008.

Finlayson-Pitts, B.J., Wingen, L.M., Sumner, A.L., Syomin, D., and Ramazan, K.A.: The heterogeneous hydrolysis of NO_2 in laboratory systems and in outdoor and indoor atmospheres: An integrated mechanism, Phys. Chem. Chem. Phys., 5, 223–242, doi:10.1039/b208564j, 2003.

France, J.L., King, M.D., Frey, M.M., Erbland, J., Picard, G., Preunkert, S., MacArthur, A., and Savarino, J.: Snow optical properties at Dome C, Antarctica; implications for snow emissions and snow chemistry of reactive nitrogen, Atmos. Chem. Phys., 11, 9787-9801, 2011.

Frey, M.M., Brough, N., France, J.L., Anderson, P.S., Traulle, O., King, M.D., Jones, A.E., Wolff, E.W., and Savarino, J.: The diurnal variability of atmospheric nitrogen oxides (NO and NO_2) above the Antarctic Plateau driven by atmospheric stability and snow emissions, Atmos. Chem. Phys., 13, 3045–3062, doi:10.5194/acp-13-3045-2013, 2013.

Frey, M.M., Roscoe, H.K., Kukui, S., Savarino, J., France, J.L., King, M.D., Legrand, M., and Preunkert, S.: Atmospheric nitrogen oxides (NO and NO_2) at Dome C, East Antarctica, during the OPALE campaign, this issue.

Gaffney, J.S., Marley, N.A., and Cunningham, M.M.: Measurement of the absorption constants for nitrate in water between 270 and 335 nm, Environ. Sci. Technol., 25, 207–209, 1992.

Gallet, J.-C., Dominé, F., Arnaud, L., Picard, G., and Savarino, J.: Vertical profile of the specific surface area and density of the snow at Dome C and on a transect to Dumont D'Urville, Antarctica – albedo calculations and comparison to remote sensing products, The Cryosphere, 5, 631–649, doi:10.5194/tc-5-631-2011, 2011.

Gallée, H. and Gorodetskaya, I.: Validation of a limited area model over Dome C, Antarctic Plateau, during winter, 34, 61–72, Clim. Dyn., doi:10.1007/s00382-008-0499-y, 2008.

Gallée, H., Preunkert, S., Jourdain, B., Argentini, S., Frey, M., Genthon, C., Pietroni, I., Casasanta, G., and Legrand, M. : Characterization of the boundary layer at Dome C during OPALE, Atmos. Chem. Phys., this issue.

George, C., Strekowski, R.S., Kleffmann, J., Stemmler, K., and Ammann, M.: Photoenhanced uptake of gaseous NO_2 on solid organic compounds: a photochemical source of HONO, Faraday Discuss., 130, 195–211, 2005.

Grannas, A.M., Jones, A.E., Dibb, J., Ammann, M., Anastasio, C., Beine, H.J., Bergin, M., Bottenheim, J., Boxe, C.S., Carver, G., Chen, G., Crawford, J.H., Domine´, F., Frey, M.M., Guzmán, M.I., Heard, D.E., Helmig, D., Hoffmann, M.R., Honrath, R.E., Huey, L.G., Hutterli, M., Jacobi, H.W., Klán, P., Lefer, B., McConnell, J., Plane, J., Sander, R., Savarino, J., Shepson, P.B., Simpson, W.R., Sodeau, J.R., von Glasow, R., Weller, R., Wolff, E.W., and Zhu, T.: An overview of snow photochemistry: evidence, mechanisms and impacts, Atmos. Chem. Phys., 7, 4329–4373, http://www.atmos-chem-phys.net/7/4329/2007/, 2007.

Gutzwiller, L., Arens, F., Baltensperger, U., Gäggeler, H.W., and Ammann, M.: Significance of semivolatile diesel exhaust organics for secondary HONO formation, Environ. Sci. Technol., 36, 677-682, doi:10.1021/es015673b, 2002.

Heland, J., Kleffmann, J., Kurtenbach, R., and Wiesen, P. : A new instrument to measure gaseous nitrous acid (HONO) in the atmosphere, Environ. Sci. Technol., 35(15), 3207-3212, doi:10.1021/es000303t, 2001.

Hudson, S.R., Warren, S.G., Brandt, R.E., Grenfell, T.C., and Six, D. : Spectral bidirectional reflectance of Antarctic snow: Measurements and parameterization, J. Geophys. Res., 111, D18106, doi:10.1029/2006JD007290, 2006.

Jones, A.E., Weller, R., Wolff, E.W., and Jacobi, H.-W.: Speciation and rate of photochemical NO and NO_2 production in Antarctic snow, Geophys. Res. Lett., 27(3), 345–348, 2000.

Kerbrat, M., Legrand, M., Preunkert, S., Gallée, H., and Kleffmann, J.: Nitrous Acid at Concordia on the East Antarctic Plateau and its transport to the coastal site of Dumont d'Urville, J. Geophys. Res., 117, D08303, doi:10.1029/2011JD017149, 2012.

Kirchstetter, T.W., Harley, R.A., and Littlejohn, D.: Measurement of nitrous acid in motor vehicle exhaust, Environ. Sci. Technol., 30, 2843-2849, 10.1021/es960135y, 1996.

Kleffmann, J., Heland, J., Kurtenbach, R., Lorzer, J., and Wiesen, P.: A new instrument (LOPAP) for the detection of nitrous acid (HONO), Environ. Sci. Pollut. Res., (Sp. Iss. 4), 48–54, 2002.

Kleffmann, J., and Wiesen, P. : Technical Note: Quantification of interferences of wet chemical HONO LOPAP measurements under simulated polar conditions, Atmos. Chem. Phys., 8, 6813–6822, www.atmos-chem-phys.net/8/6813/2008/, 2008.

Kokhanovsky, A.A., and Zege, E.P.: Scattering optics of snow, Appl. Optics, 43, 1589–1602, 2004.

Kukui, A., Legrand, M., Ancellet, G., Gros, V., Bekki, S., Sarda-Estève, R., Loisil, R., and Preunkert, S.: Measurements of OH and RO_2 radicals at the coastal Antarctic site of Dumont d'Urville (East Antarctica) in summer, J. Geophys. Res., doi:10.1029/2012JD017614, 2012.

Kukui, A., Legrand, M., Preunkert, S., Frey, M., Loisil, R., Gil Roca, J., Jourdain, B., King, M., France, J., and Ancellet, G.: OH and RO_2 measurements at Dome C, East Antarctica, Atmos. Chem. Phys., this issue.

Kurtenbach, R., Becker, K.H., Gomes, J.A.G., Kleffmann, J., Lorzer, J.C., Spittler, M., Wiesen, P., Ackermann, R., Geyer, A., and Platt, U.: Investigations of emissions and heterogeneous formation of HONO in a road traffic tunnel, Atmos. Environ., 35, 3385-3394, 10.1016/s1352- 2310(01)00138-8, 2001.

Legrand M., Preunkert, S., Jourdain, B., Gallée, H., Goutail, F., Weller, R., and Savarino, J.: Year round record of surface ozone at coastal (Dumont d'Urville) and inland (Concordia) sites in East Antarctica, J. Geophys. Res., 114, D20306, doi:10.1029/2008JD011667, 2009.

Legrand, M., Preunkert, S., Jourdain, B., Guilhermet, J., Faïn, X., Alekhina, I., and Petit, J.R. : Water-soluble organic carbon in snow and ice deposited at Alpine, Greenland, and Antarctic sites: A critical review of available data and their atmospheric relevance, Clim. Past, 9, 2195-2211, doi:10.5194/cp-9-2195-2013, 2013.

Li, X., Rohrer, F., Hofzumahaus, A., Brauers, T., Häseler, R., Bohn, B., Broch, S., Fuchs, H., Gomm, S., Holland, F., Jäger, J., Kaiser, J., Keutsch, F. N., Lohse, I., Lu, K., Tillmann, R., Wegener, R., Wolfe, G. M., Mentel, T. F., Kiendler-Scharr, A., and Wahner, A.: Missing Gas-Phase Source of HONO Inferred from Zeppelin Measurements in the Troposphere, Science, 344, 292-296, 2014.

Liao, W., Case, A.T., Mastromarino, J., Tan, D., and Dibb, J.E. : Observations of HONO by laser-induced fluorescence at the South Pole during ANTCI 2003, Geophys. Res. Lett., 33, L09810, doi:10.1029/2005GL025470, 2006.

Mauldin, R.L., Eisele, F.L., Tanner, D.J., Kosciuch, E., Shetter, R., Lefer, B., Hall, S.R., Nowak, J.B., Buhr, M., Chen, G., Wang, P., and Davis, D. : Measurements of OH, H_2SO_4, and MSA at the South Pole during ISCAT, Atmos. Environ., 28, 3629-3632, 2001a.

Mauldin III, R.L., Eisele, F.L., Cantrell, C.A., Koscisuch, E., Ridley, B.A., Lefer, B., Tanner, D.J., Nowak, J.B., Chen, G., Wang, L., and Davis, D. : Measurements of OH aboard the ASA P-3 during PEM-Tropics B., J. Geophys. Res., 106, 32,657-32,666, 2001b.

Meusinger, C., Berhanu, T.A., Erbland, J., Savarino, J., and Johnson, M.S. : Laboratory Study of Nitrate Photolysis in Antarctic Snow, Part 1: Observed Quantum Yield, Domain of Photolysis and Secondary Chemistry, J. Chem. Phys., 140, 244305, 2014.

Preunkert S., Ancellet, G., Legrand, M., Kukui, A., Kerbrat, M., Sarda-Estève, R., Gros, V., and Jourdain, B.: Oxidant Production over Antarctic Land and its Export (OPALE) project: An overview of the 2010-2011 summer campaign, J. Geophys. Res., doi:10.1029/2011JD017145, 2012.

Regimbal, J., and Mozurkewich, M.: Peroxynitric acid decay mechanisms and kinetics at low pH, J. Phys. Chem. A, 101, 8822–8829, 1997.

Sander, S.P., and Peterson, A.E.: Kinetics of the reaction HO_2+NO_2+M→HO_2NO_2+M, J. Phys. Chem., 88, 166-1571, 1984.

Sander, S.P., J. Abbatt, J.R. Barker, J.B. Burkholder, R.R. Friedl, D.M. Golden, R.E. Huie, C. E. Kolb, M.J. Kurylo, G.K. Moortgat, V.L. Orkin and P.H. Wine : "Chemical Kinetics and Photochemical Data for Use in Atmospheric Studies, Evaluation No. 17," JPL Publication 10 June 2011, Jet Propulsion Laboratory, Pasadena, http://jpldataeval.jpl.nasa.gov, 2011.

Slusher, D.L., Huey, L.G., Tanner, D.J., Chen, G., Davis, D.D., Buhr, M., Nowak, J.B., Eisele, F., Kosciuch, E., Mauldin, R.L., Lefer, B.L., Shetter, R.E., and Dibb, J.E.: Measurements of pernitric acid at the South Pole during ISCAT 2000, Geophys. Res. Lett., 29, 2011, doi:10.1029/2002GL015703, 2002.

Slusher, D.L., Neff, W.D., Kim, S., Huey, L.G., Wang, Y., Zeng, T., Tanner, D.J., Blake, D. R., Beyersdorf, A., Lefer, B.L., Crawford, J.H., Eisele, F.L., Mauldin, R.L., Kosciuch, E., Buhr, M.P., Wallace, H.W., and Davis, D.D.: Atmospheric chemistry results from the ANTCI 2005 Antarctic plateau airborne study, J. Geophys. Res. Atmos., 115, D07304, doi:10.1029/2009JD012605, 2010.

Ulrich, T., Ammann, M., Leutwyler, S., and Bartels-Rausch, T.: The adsorption of peroxynitric acid on ice between 230 K and 253 K, Atmos. Chem. Phys., 12, 1833-1845, 10.5194/acp-12-1833-2012, 2012.

Villena, G., Wiesen, P., Cantrell, C.A., Flocke, F., Fried, A., Hall, S.R., Hornbrook, R.S., Knapp, D., Kosciuch, E., Mauldin III, R.L., McGrath, J.A., Montzka, D., Richter, D., Ullmann, K., Walega, J., Weibring, P., Weinheimer, A., Staebler, R.M., Liao, J., Huey, L.G., and Kleffmann, J. : Nitrous acid (HONO) during polar spring in Barrow, Alaska: A net source of OH radicals?, J. Geophys. Res., 116, D00R07, doi:10.1029/2011JD016643, 2011.

Table 1. Results of irradiation experiments performed at the BAS laboratory on three different surface snows collected at Concordia. S1 and S2 are upper surface snows collected between 0 and 1 cm, S3 is the surface snow collected between 0 and 12 cm depth. The acidity is calculated by checking the balance between anions and cations (see Sect. 2.2). DL refers to detection limit and N.C. means non-calculated value.

Snow type	Date in 2013	Wavelengths λ >	T (°C)	HONO (pptv)	NO_x (pptv)	HONO/ NO_x	NO_3^- (ppb)	H^+ ($\mu Eq\ L^{-1}$)
S1	23 Jan	295 nm	-15	117 ± 5	137 ± 20	0.85 ± 0.1	1428	29.4
S1	24 Jan	295 nm	-15.5	120 ± 3	129 ± 16	0.93 ± 0.1	1428	29.4
S1	24 Jan	320 nm	-16	47 ± 1	67 ± 12	0.70 ± 0.1	1428	29.4
S1	24 Jan	385 nm	-16	< 3	< DL	N.C.	1428	29.4
S2	23 Apr	295 nm	-13	124 ± 1	162 ± 14	0.77 ± 0.1	1344	24.0
S2	23 Apr	295 nm	-22.5	86 ± 3	167 ± 40	0.52 ± 0.1	1344	24.0
S2	23 Apr	295 nm	-34	56 ± 1	210 ± 50	0.27 ± 0.2	1344	24.0
S3	25 Apr	295 nm	-21	15 ± 2	47 ± 27	0.32 ± 0.15	157	4.0

Figures

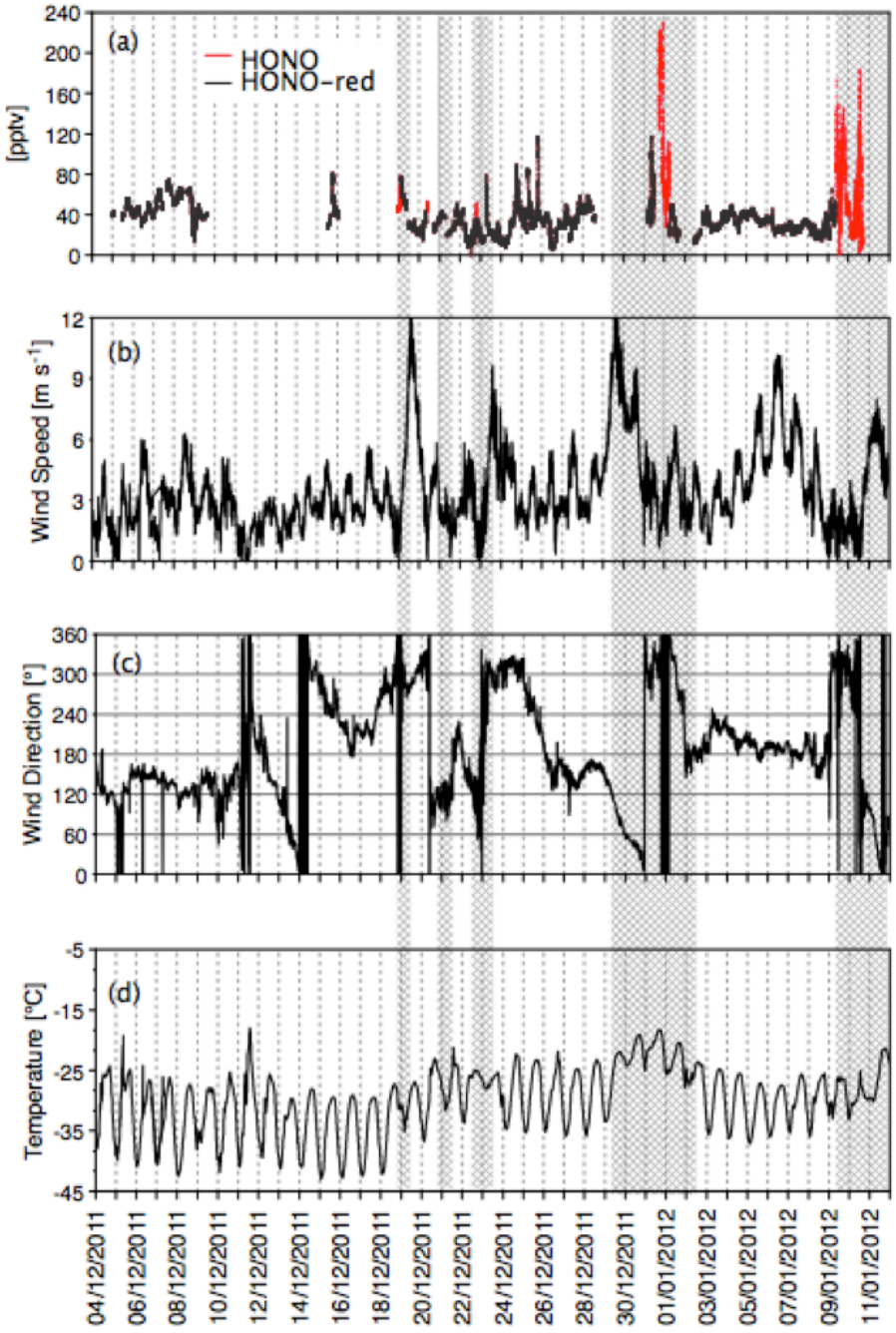

Fig. 1. Summer 2011/2012 time series of HONO mixing ratios (1 min average) (a), wind conditions (b and c) and temperatures (d) at Concordia. Red points of the HONO record refer to time periods during which contamination from the station was possible with the wind was blowing from North (from 10°W to 60°E sector, see Sect. 2.2). Grey backgrounds indicate time period of overcast weather.

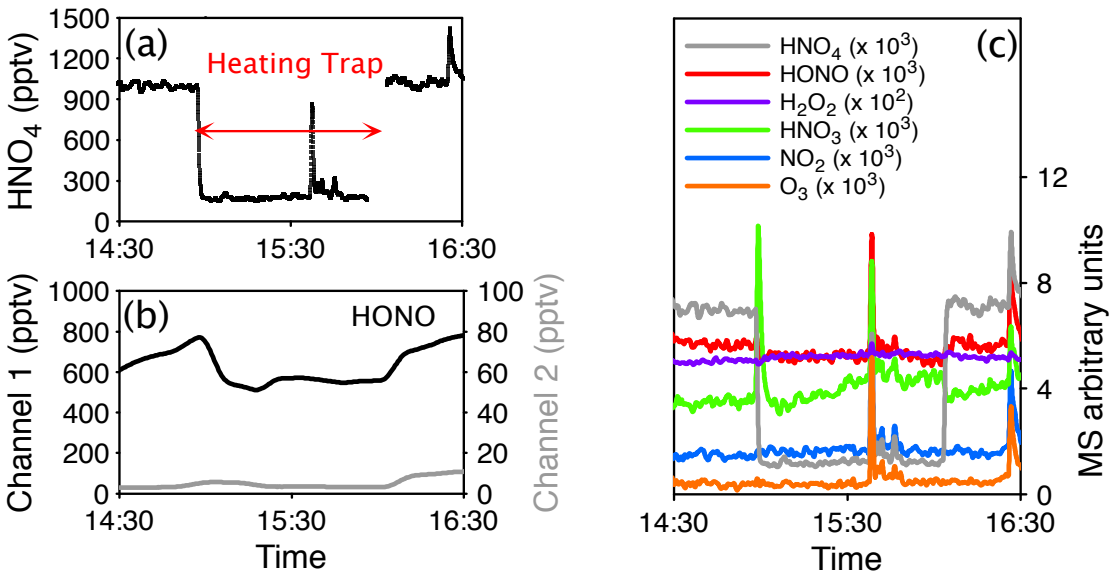

Fig. 2. The experiment carried out at the PSI laboratory in view to investigate the interference of HNO_4 on HONO measurements made with the LOPAP deployed during the two Concordia campaigns. Left: Time traces of HNO_4 (top) and of the two LOPAP channels (bottom). Time at which the heating trap was activated is shown with a red horizontal arrow. Right: Intensities of NO_2, HONO, HNO_3, HNO_4, O_3, and H_2O_2 traces as detected by the mass spectrometer (see Sect. 2.4). Heating the gas mixture to 100°C leads to a sharp decrease in HNO_4 and a small increase of HNO_3 intensities. O_3 and H_2O_2 remain stable whereas a very small decrease of HONO is detectable.

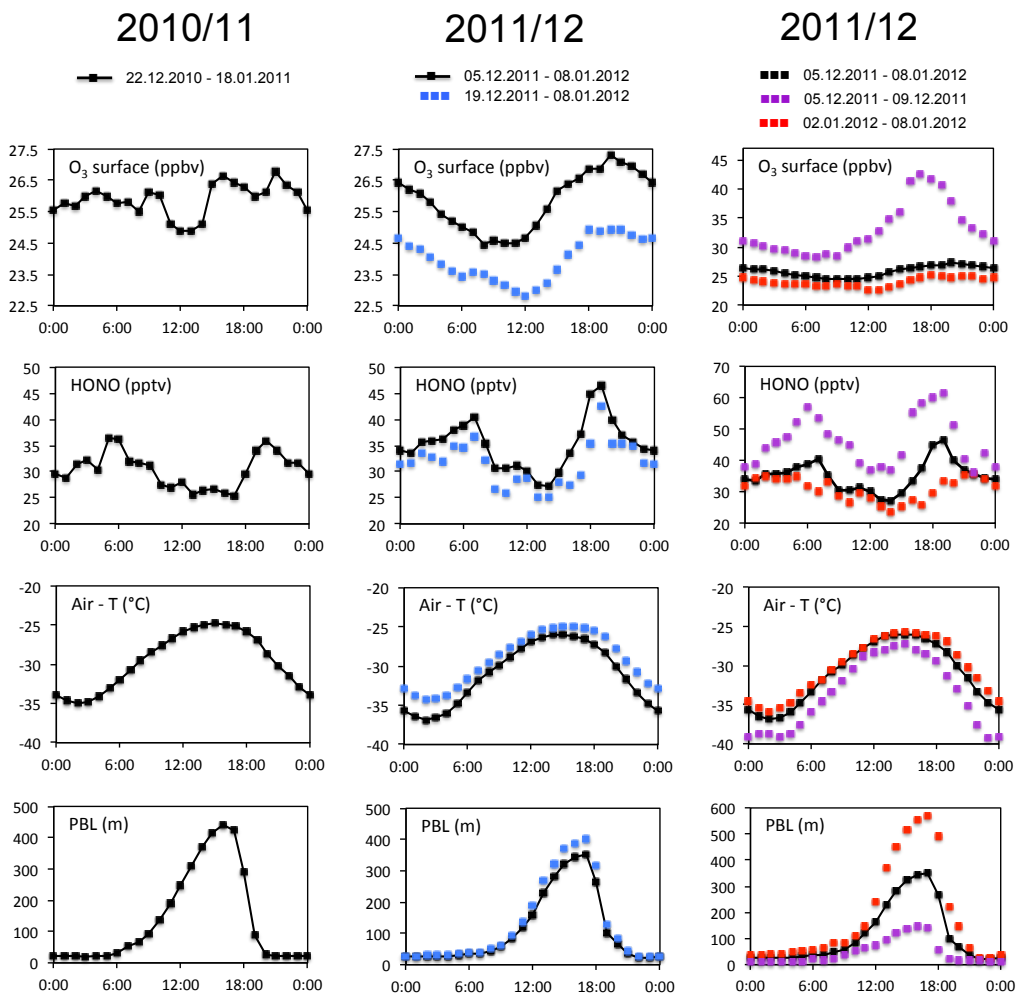

Fig. 3. Left and central: From top to bottom, diurnal changes of surface ozone mixing ratio, HONO mixing ratio, air temperature and PBL height simulated by the MAR model (see Sect. 5) at Concordia over the entire period of measurements in 2010/2011 (left) and 2011/20112 central (black dots). The blue dots reported for the 2011/2012 summer correspond to the period between December 19th 2011 and January 8th 2012. Right: Same as left and central but for the entire 2011/2012 period (black dots), at the beginning (early December, violet dots) and the end (red dots) of the period. Note the use of different vertical scales for right compared to left and central panels.

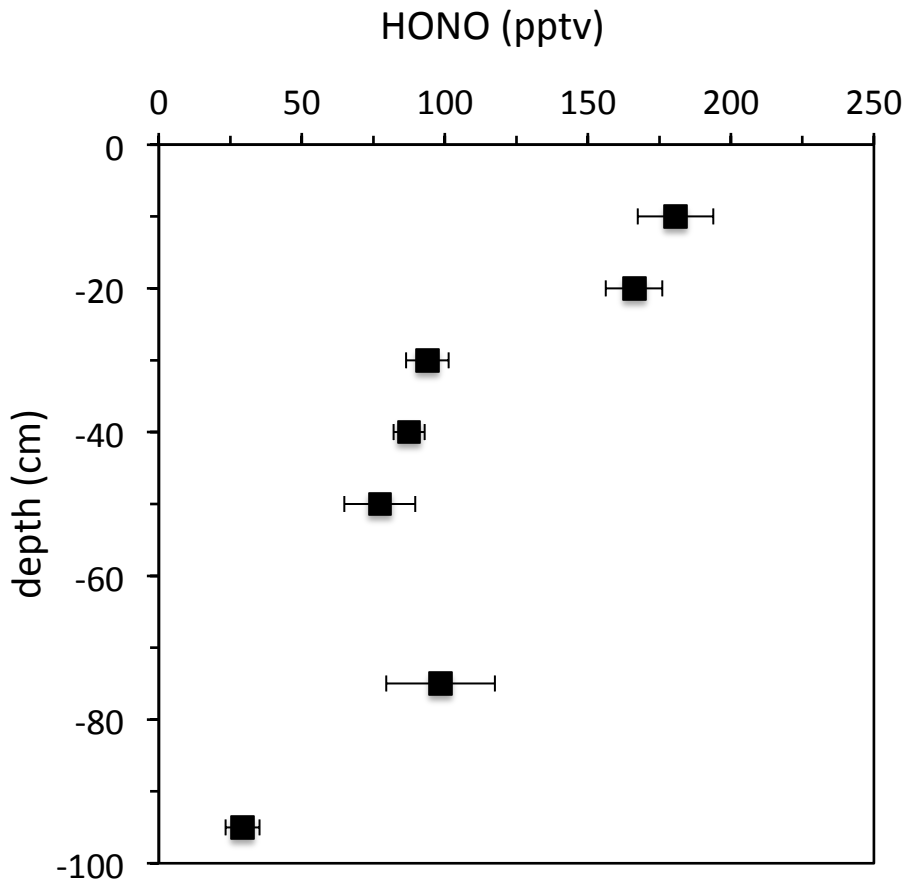

Fig. 4. Firn air mixing ratios of HONO down to 1 m depth measured at Concordia at 13 January 2012.

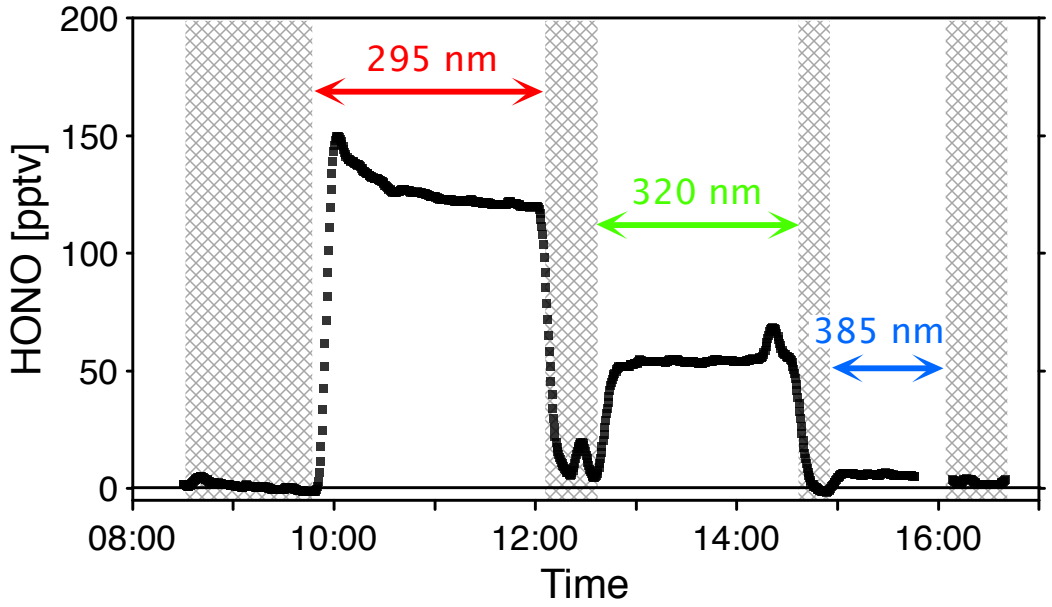

Fig. 5. Photochemical release of HONO from a surface snow collected at Concordia when irradiating it at a temperature of -16°C (see Table 1) and inserting filters with cut-on points at 295 nm, 320 nm, and 385 nm on the Xenon-arc lamp (see Sect. 4). Vertical grey bands correspond to periods over which the lamp was switched off.

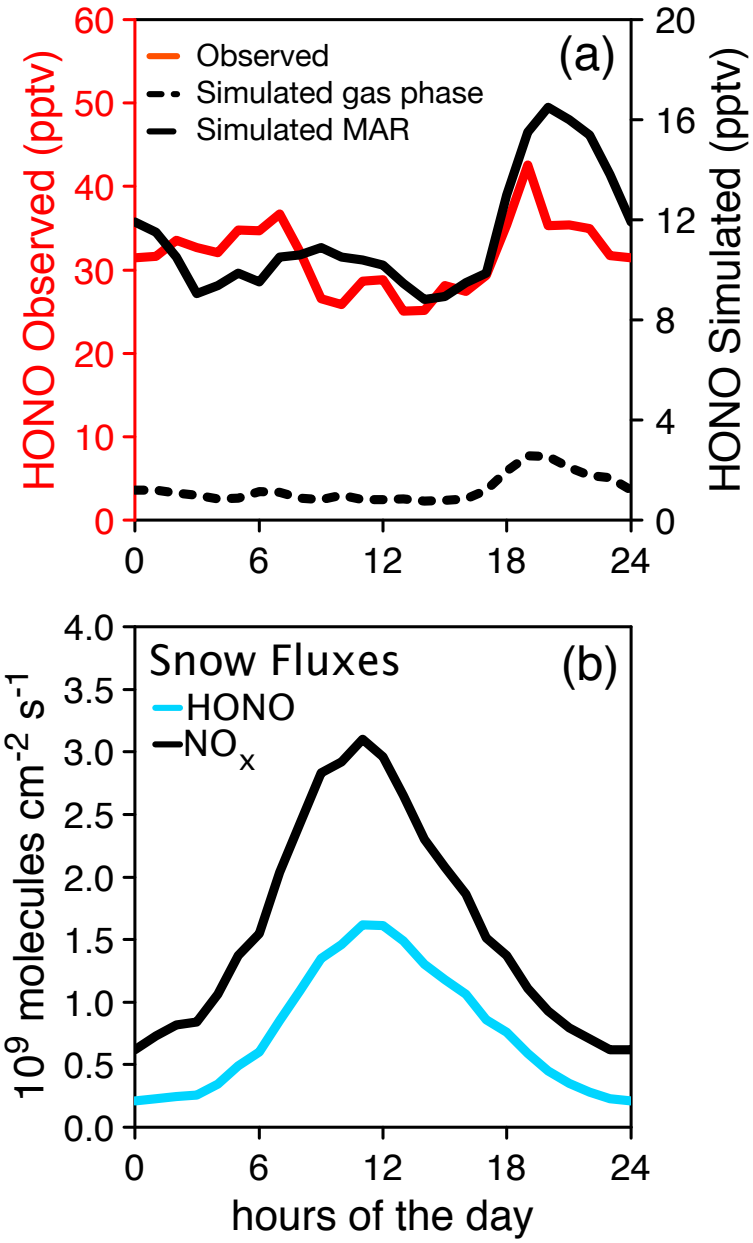

Fig. 6. Top : Measured (red line) versus simulated (black lines) (see Sect. 5) diurnal cycles of HONO mixing ratio at 1 m height. Note the use of a different vertical scale for observations (left) and simulations (right). The black dashed line is the simulation made when considering only the gas phase production of HONO from NO (without snow emissions). Bottom : Diurnal NO_x snow source derived from field observations at Concordia (Frey et al., this issue) together with an estimated emission of HONO from snow based on laboratory snow irradiation experiments (see Sect. 4).